Engl., **18**, 62 (1979).
9. W. H. Pirkle, T. C. Pochapsky, G. S. Mahler, D. E. Corey, D. S. Reno, and D. M. Alessi, *J. Am. Chem. Soc.*, **108**, 5627 (1986).
10. (a) S. K. Burley and G. A. Petsko, *Science*, **229**, 23 (1985); (b) J. N. Herron, X. He, M. L. Mason, E. W. Voss, and A. B. Edmundson, *Proteins*, **5**, 271 (1989); (c) A. V. Muehldorf, D. Van Engen, J. C. Wainer, and A. D. Hamilton, *J. Am. Chem. Soc.*, **110**, 6561 (1988); (d) I. Z. Siemion, *Z. Naturforsch, B*, **45**, 1324 (1990).

The Rheological and Mechanical Model for Relaxation Spectra of Polydisperse Polymers

Nam Jeong Kim*, Eung Ryul Kim, and Sang Joon Hahn

Department of Chemistry, Hanyang University, Seoul 133-791
**Department of Chemistry, Korean Sahmyook University, Seoul 139-742.* *Received March 20, 1992*

The theoretical equation for the relaxation spectrum of nonlinear viscoelastic polymeric material was derived from the Ree-Eyring and Maxwell non-Newtonian model. This model consists of infinite number of hyperbolic sine law Maxwell elements coupled in parallel plus a spring without a dashpot. Infinite number of nonlinear viscoelastic Maxwell elements can be used by specifying distribution of relaxation times, hole volumes, molecular weights, crystallite size and conformational size, etc. The experimentals of stress relaxation were carried out using the tensile tester with the solvent chamber. The relaxation spectra of nylon 6 filament fibers in various electrolytic solutions were obtained by applying the experimental stress relaxation curves to the theoretical equation of relaxation spectrum. The determination of relaxation spectra was performed from computer calculation.

Introduction

The relaxation spectra for the linear viscoelastic polymeric materials have been reported[1-4]. However, the theoretical and phenomenological analysis for the relaxation spectrum of nonlinear viscoelasticity has not been performed sufficiently, due to the theoretical treatments involving more complicated function. The viscoelastic behavior of polymeric materials at modest to large deformation is complicated by material nonlinearities. These nonlinearities are thought to arise from the distribution in molecular weights, crystallite size, conformational size and relaxation times of flow segments.

Viscous interfaces also play a significant role in determining the time-dependent properties of bone[5], for which a logarithmic spectrum has been used successfully in constructing a constitutive equation[6]. The logarithmic relaxation spectrum may be of use in describing system in which viscoelastic behavior arisen from motion along viscous interfaces in an elastic matrix. Although it is relatively easy to obtain the viscoelastic functions from the relaxation spectra, the reverse process is difficult, and usually involves successive approximations of some kind. For these reasons, a variety of approximation methods[7,8] have been developed for performing such calculation. Generally, the approximation methods have an analytical foundation based on the properties of the integrands of the corresponding exact equation. Such an integrand is usually the product of the viscoelastic function initially known and an additional dimensionless intensity functions. If, within a particular zone of viscoelastic behavior, an empirical equation can be used to fit a viscoelastic function, an exact expression for the corresponding spectrum and sometimes be derived as shown by Smith[9].

In this work, the theoretical equation for the relaxation spectrum of nonlinear viscoelastic materials was derived from the Ree-Eyring and Maxwell non-Newtonian model. This model consists of infinite number of hyperbolic sine law Maxwell elements coupled in paralled plus a spring without a dashpot. Each non-Newtonian Maxwell element can be specified by relaxation time and intrinsic strain modulus, and in the general case infinite number of nonlinear viscoelastic Maxwell elements can be used by specifying a distribution of relaxation times, hole volumes and molecalar weights. The relaxation spectra of the solid polymers were obtained by applying the experimental stress relaxation curves to the theoretical relaxation spectrum equation. It is observed that the relaxation spectra of these samples are directly related to the distribution of viscosities, activation free energies, relaxation times and molecalar weights.

Theory

The Ree-Eyring and Maxwell Non-Newtonian Model. The Ree-Eyring and Maxwell non-Newtonian model put forward by Ree, Hahn and his colleagues, shown in Figure 1. This model consists of a spring and infinite number of non-Newtonian Maxwell elements coupled in parallel. As can be seen, it necessarily possesses many relaxation times and shear moduluses. For real viscoelastic polymeric materials, we postulate the existence of a continuous spectrum of relaxation times. The concept that a continuous distribution of relaxation times should be required to represent the

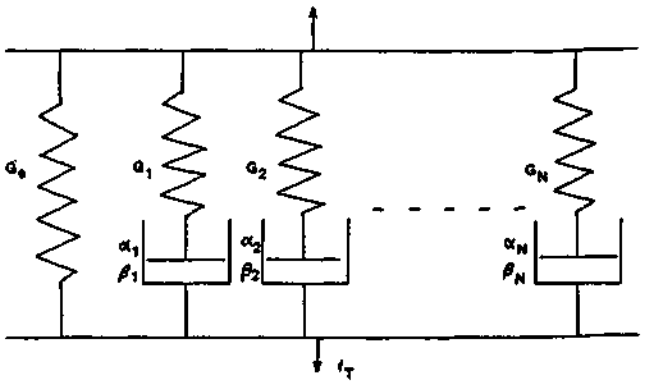

Figure 1. The ree-eyring and maxwell non-newtonian model.

behavior of real system would seem to follow quite naturally since we already know that real polymeric system also exhibit distribution in molecular weight, hole distance of flow segments, crystallite size, conformational size, etc.

In this model, the dashpots follow a hyperbolic sine law of non-Newtonian viscosity[10,11], we have strain rate of dashpot;

$$\frac{dS}{dt}=\frac{1}{\beta_i}\sin h(\alpha_i f_i) \tag{1}$$

Whereas the springs follow Hooke's law, so that the strain and the strain rate of springs are given by

$$S=\frac{f_i}{G_i} \tag{2}$$

$$\frac{dS}{dt}=\frac{1}{G_i}\frac{df_i}{dt} \tag{3}$$

Where G_i denote Young's modulus

For the hyperbolic sine non-Newtonian Maxwell elements of this model, with springs of modulus G_i and stress f_i, we have:

$$\frac{dS}{dt}=\sum_{i=1}^{N}\frac{1}{G_i}\frac{df_i}{dt}+\sum_{i=1}^{N}\frac{1}{\beta_i}\sin h(\alpha_i f_i) \tag{4}$$

For the spring of equilibrium stress f_e, we have strain rate

$$\frac{dS}{dt}=\frac{1}{G_e}\frac{df_e}{dt} \tag{5}$$

The total stress $f(t)$ is the sum of all the partial stresses, therefore:

$$f(t)=f_e+\sum_{i=1}^{N}f_i \tag{6}$$

On differentiation by time t, this gives:

$$\frac{df(t)}{dt}=\frac{df_e}{dt}+\frac{d\sum_{i=1}^{N}f_i}{dt} \tag{7}$$

From Eq. (4), (5), and (7), we have:

$$\frac{df(t)}{dt}=G_e\frac{dS}{dt}+\sum_{i=1}^{N}G_i\frac{dS}{dt}-\sum_{i=1}^{N}\frac{G_i}{\beta_i}\sin h(\alpha_i f_i)$$

$$=(G_e+\sum_{i=1}^{N}G_i)\frac{dS}{dt}-\sum_{i=1}^{N}\frac{G_i}{\beta_i}\sin h\alpha_i(f(t)f_e) \tag{8}$$

The Theoretical Equation for Relaxation Spectrum. In stress relaxation with constant strain Sc, we have $\frac{dS}{dt}=0$, and Eq. (8) becomes:

$$\frac{df(t)}{dt}=-\sum_{i=1}^{N}\frac{G_i}{\beta_i}\sin h\,\alpha_i(f(t)G_eS_c) \tag{9}$$

From which:

$$\sum_{i=1}^{N}\frac{df(t)}{\sin h\alpha_i(f_T-G_eS_c)}=-\sum_{i=1}^{N}\frac{G_i}{\beta_i}dt \tag{10}$$

One integration, this gives:

$$\ln\tan h\sum_{i=1}^{N}\alpha_i(f(t)-G_eS_c)/2=-\sum_{i=1}^{N}G_i\frac{1}{\beta_i}t+C \tag{11}$$

As boundary conditions, initial stress $f_o=(G_e+\sum_{i=1}^{N}G_i)S_c$ at $t=0$, and final stress $f_e=G_eS_c$ at $t=\infty$ can be applied, since the stresses on non-Newtonian Maxwell elements decay very slowly. The integral constant is given by the boundary conditions, we get:

$$C=\ln\tan h\sum_{i=1}^{N}\alpha_i(f_o-f_e)/2 \tag{12}$$

By substituting Eq. (12) into (11), we obtain the equation for stress relaxation.

$$f(t)=f_e+\sum_{i=1}^{N}\frac{2}{\alpha_i}\tan h^{-1}\left[\tan(\alpha_i(f_o-f_e)/2)\exp\left\{\frac{-\alpha_iG_i}{\beta_i}t\right\}\right] \tag{13}$$

Introducing the approximation $\tan h^{-1}x\simeq x(x\ll 1)$

$$f(t)=f_e+\sum_{i=1}^{N}\frac{2}{\alpha_i}\tan h\left[(\alpha_i(f_o-f_e)/2)\exp\left\{\frac{-\alpha_iG_i}{\beta_i}t\right\}\right] \tag{14}$$

If the number of the hyperbolic sine law non-Newtonian elements is allowed to become infinite with the characteristic parameter becoming a continuous function of the relaxation time, the summation over the differential elements of the model can be replaced by an integration over all relaxation times.

Assuming that relaxation times β_i are continuous distribution, we obtain the following integral equation.

$$f(t)=f_e+\int_0^{\infty}\frac{2}{\alpha}\tan h(\alpha(f_o-f_e)/2)\exp\left\{-\frac{\alpha G}{\beta}t\right\}d\beta \tag{15}$$

Since the relaxation modulus $G(t)=f(t)/S_c$, we find that we have developed a expression suitable for representing the time dependence of the relaxation modulus

$$G(t)=G_e+\int_0^{\infty}\frac{2}{S_c\alpha}\tan h(\alpha(f_o-f_e)/2)\exp\left\{-\frac{\alpha G}{\beta}t\right\}d\beta \tag{16}$$

Expressing by the distribution of the relaxation time, $G(\beta)$

$$G(\beta)=\frac{2}{S_c\alpha}\tan h(\alpha(f_o-f_e)/2) \tag{17}$$

$$G(t)=G_e+\int_0^{\infty}G(\beta)\exp\left\{-\frac{\alpha G}{\beta}t\right\}d\beta \tag{18}$$

The function $G(\beta)$ is reffered to as the relaxation spectrum. In practice $G(\beta)$ is determined from experimental data on

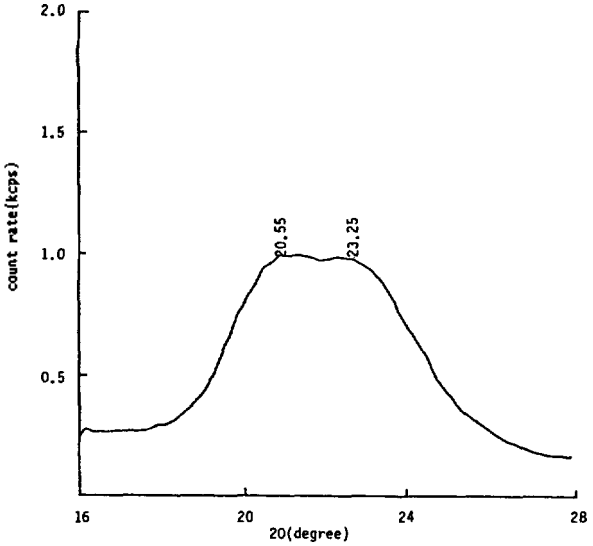

Figure 2. X-ray diffraction pattern of ordinary nylon 6 filament fiber.

$G(t)$. If the relaxation modulus data could be represented analytically, an analytic function for $G(\beta)$ could be obtained since Eq. (18) is of the Laplace transform type.

In practice, it has been found more convenient to use a logarithmic time scale. In addition to the distribution $G(\beta)$, a new relaxation time spectrum $H(\beta)$ is now simply defined as

$$G(\beta)=H(\beta)/\beta \tag{19}$$

where $H(\beta)d(\ln\beta)$ gives the contribution to the stress relaxation associated with relaxation times between $\ln\beta$ and $\ln\beta+d(\ln\beta)$. For the contribution spectrum, Eq. (18) becomes

$$G(t)=G_e+\int_{-\infty}^{\infty} H(\beta)\exp\left(-\frac{\alpha G}{\beta}t\right)d\ln\beta \tag{20}$$

$$H(\beta)=\frac{2}{S_c\alpha}\tan h\,[\alpha(f_o-f_c)/2] \tag{21}$$

The constant G_e is added because of the contribution to the spectrum with $\beta=\infty$, for viscoelastic solids.

Experimental

Material. The polydisperse Nylon 6 monofilament fiber of 67 denier was provided by Dongyang Nylon Co., Inc., Korea. The degrees of crystallinity and the orientation factor of crystalline size (f_c) were avaiiable by the wide angle X-ray diffractometer of following conditions[12] (Device: wide angle goniometer, Step width: 0.05 degree, Fixed time: 2 second, Target: Cu($K\alpha$ radiation source)). The X-ray diffraction pattern of Nylon 6 is shown in Figure 2. The degrees of crystallinity and the orientation factor (f_c) of Nylon 6 mono fiber were obtained as about 58.26% and 0.835, respectively. Nylon 6 fiber samples were stored in the solvents of distilled water, 0.5 M KCl, 0.5 M $BaCl_2$ and 0.5 M $AlCl_3$ aqueous solution at various temperatures of 10℃, 20℃, 30℃, and 40℃ for at least 1 hour prior to the measurements.

Apparatus and Measurement. The apparatus used in this work is a tensile tester with the solvent chamber connected to the low jaw. The solvent chamber was equipped with a water bath which could be kept at a desired temperature by automatic system (Julabo F20), and the water bath was thermostatically controlled within ± 0.05℃. The Nylon 6 sample was fixed by two jaws: the upper jaw was fixed to the load cell (transducer type-UK-LK Model No 5550318) and lower jaw free to move by crosshead. The crosshead can be moved by the Vexta stepping motor (model pH 266-02GK, Oriental Motor co., Japan) has constant velocity.

In this experiment the test length was 50 mm, and the elongation rate for giving constant strain of 5-20% was 50 mm/min. The constant strain was maintained for more than 3600 sec. The force on the filaments was measured by a strain gauge and plotted on a strip-chart recorder. The stress of sample was calculated from the measured cross sectional area of the filaments.

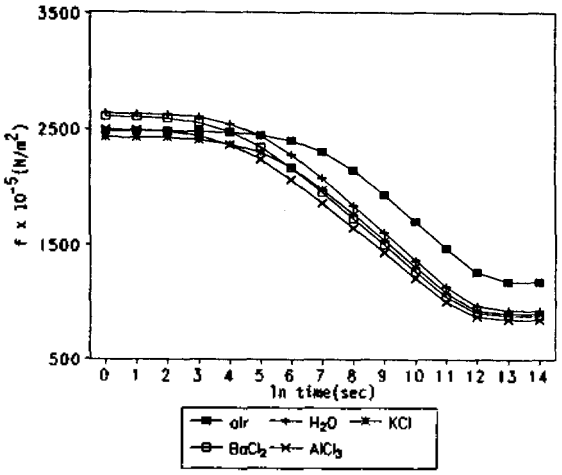

Figure 3. Stress relaxation curves of nylon 6 monofilament fibers in air, distilled water, 0.5 M KCl, 0.5 M $BaCl_2$ and 0.5 M $AlCl_3$ aqueous solution at 20℃.

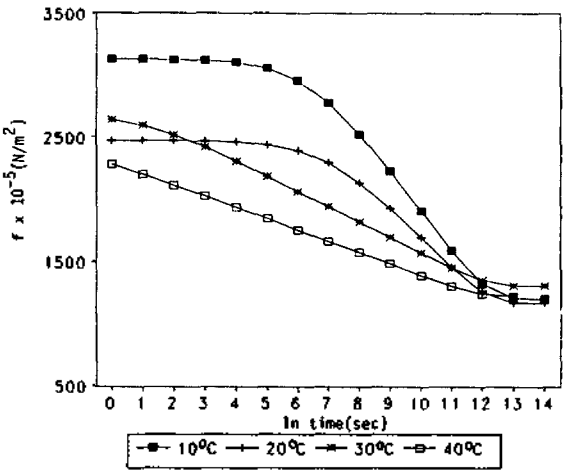

Figure 4. Stress relaxation curves of nylon 6 monofilament fibers in air at 10℃, 20℃, 30℃ and 40℃.

Results and Discussion

Stress Relaxation Curves. The stress relaxation curves

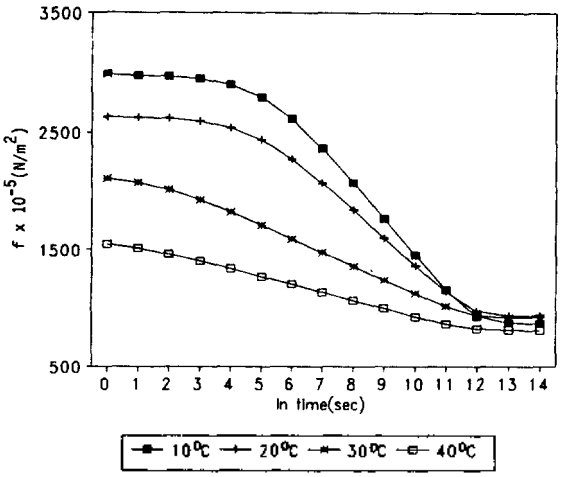

Figure 5. Stress relaxation curves of nylon 6 monofilament fibers in H_2O at 10℃, 20℃, 30℃ and 40℃.

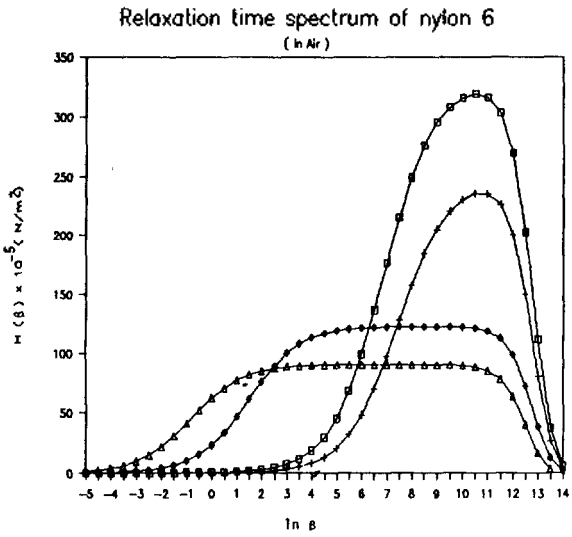

Figure 6. Relaxation time spectra of nylon 6 monofilament fibers in air at 10℃ (□), 20℃ (+), 30℃ (◇) and 40℃ (△).

of nylon 6 filament fibers in solvents at various temperatures are shown in Figure 3-5. As shown in the figures, the stress decays gradually to equilibrium value, f_e, with time at a constant strain. The quantity, f_e, is defined as at the stress $t=\infty$. Then final stress, f_e is obtained by extrapolating the straight line portion of the f *vs.* $1/t$ to zero. For this type of experiment, $ds/dt=0$, the stress due to the segment motion decays so rapidly that it is not observable. The stress on the high relaxation time segments decays very slowly, and if a limiting stress is really reached it must be due to the crystallite segments. The observed decay of stress is, therefore, due to the relaxation of bonds in segments. The observed decay of stress is, therefore, due to the relaxation of bonds in amorphous region. Of cours it will be shown that the suitable distribution of relaxation times and the molecular weight distribution, which have a natural basis in terms of molecular behavior, can also explain the observed data.

The stress at a given time decreases with increasing temperature. At higher temperatures, the tension developed at given extension becomes smaller, in keeping with the reduction in the relaxation modulus with rise in temperature. For these samples, the tension for given extension decreases linearly with temperature increase. From this experimental results, it can be seen that the flow of crystallites in amorphous region, which take part in raising the relaxation modulus[13], increase with temperature and solvation.

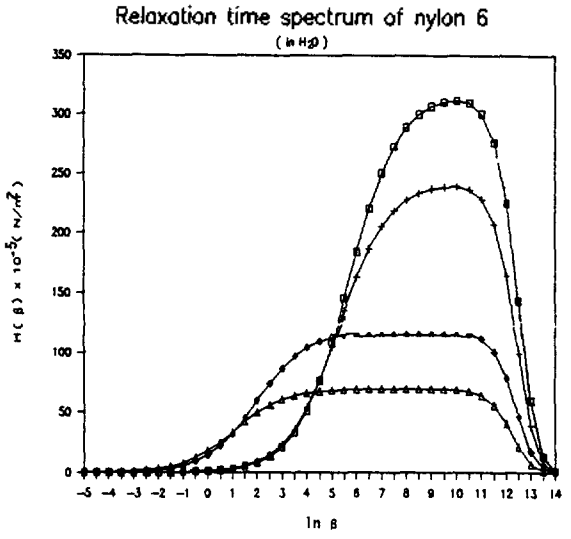

Figure 7. Relaxation time spectra of nylon 6 monofilament fiber in H_2O at 10℃ (□), 20℃ (+), 30℃ (◇) and 40℃ (△).

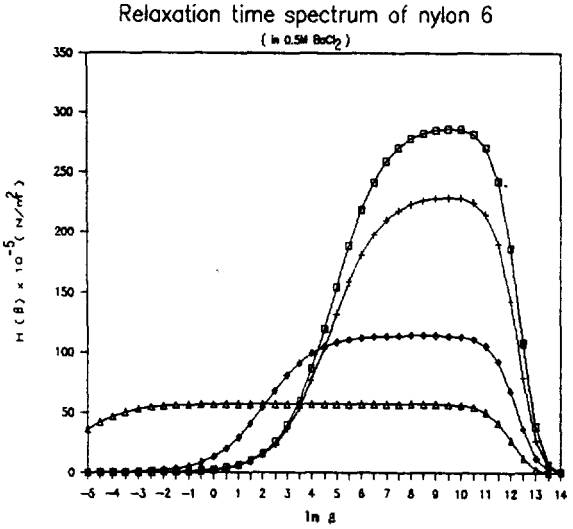

Figure 8. Relaxation time spectra of nylon 6 monofilament fiber in 0.5 M $BaCl_2$ at 10℃ (□), 20℃ (+), 30℃ (◇) and 40℃ (△).

The Relaxation Spectrum from Relaxation Modulus. The relaxation spectrum can be calculated exactly from the measured stress relaxation modulus using a Laplace transformation. The relationship between the experimentally obtained stress relaxation modulus $G(t)$ and the relaxation spectrum $H(\beta)$ was already expressed Eq. (20). If $G(t)$ is known for all values of t from zero to infinity, $H(\beta)$ can be obtained in principle. To use the Laplace transform one must know $G(t)$ over the entire time scale from $t=0$ to $t=\infty$. The all values of $G(t)$ for the entire time scale was obtained by appling the experimental stress relaxation equation of the three element non-Newtonian model as in the

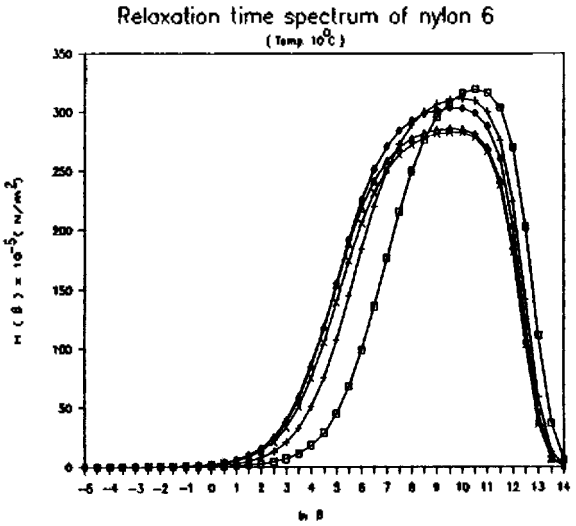

Figure 9. Relaxation time spectra of nylon 6 monofilament fibers in Air (□), H_2O (+), 0.5 M KCl (◇), 0.5 $BaCl_2$ (△) and 0.5 M $AlCl_3$ (x) at 10℃.

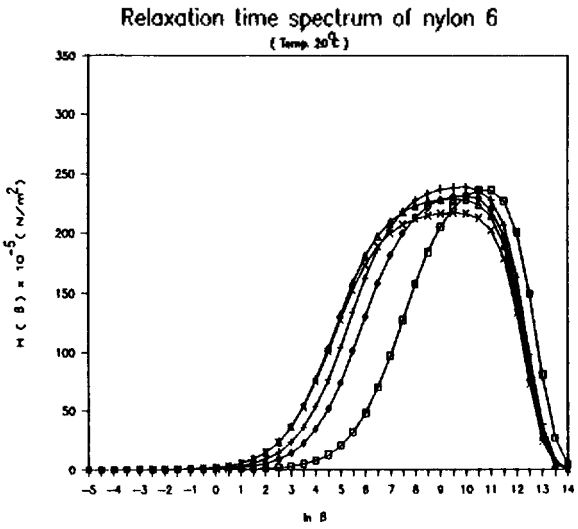

Figure 10. Relaxation time spectra of nylon 6 monofilament fiber in Air (□), H_2O (+), 0.5 M KCl (◇), 0.5 $BaCl_2$ (△) and 0.5 M $AlCl_3$ (x) at 20℃.

following[11]

$$G(t)=G_e+\frac{2}{\alpha S_c}\tan h^{-1}[\tan h(\alpha(f_o-f_c)/2]\exp\left(\frac{\alpha G_1}{\beta}t\right) \quad (22)$$

A variety of approximation methods[14-16] have been developed to evaluate the relaxation modulus $G(t)$. Most of the approximation procedures involve taking derivations either graphically or by a numerical differencing process.

For determining derivatives, the method based on numerical differencing was used. This method was performed from computer calculation after the numerical data had been obtained by the theoretical equation of the stress relaxation. In Eq. (20), the relaxation spectrum $H(\beta)$ is multiplied by the kernel function $\exp(-\alpha Gt/\beta)$ which goes from 0 at $\beta=0$ to at $\beta=\infty$. If the equation was approximated by step function going from 0 to 1 at $\beta=t$, we would have

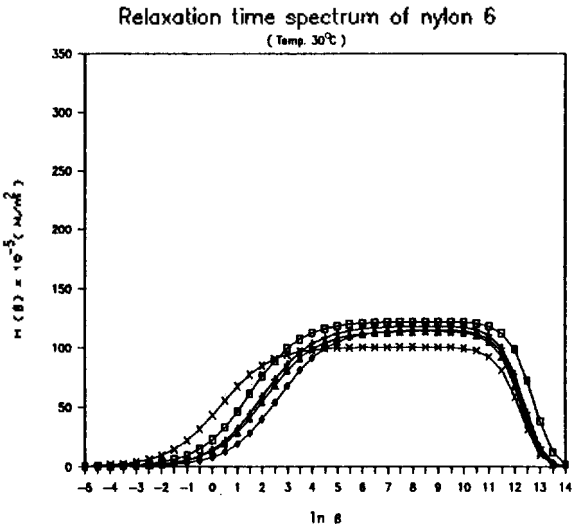

Figure 11. Relaxation time spectra of nylon 6 monofilament fiber in Air (□), H_2O (+), 0.5 M KCl (◇), 0.5 $BaCl_2$ (△) and 0.5 M $AlCl_3$ (x) at 30℃.

$$G(t)\simeq G_e+\int_{\ln t}^{\infty}H(\beta)\ d(\ln\beta) \quad (23)$$

By differentiating Eq. (23) with respect to the limit ln t,

$$-\frac{dG(t)}{d\ln t}\Big|_{t=\beta}\simeq H_1(\beta) \quad (24)$$

So the relaxation spectrum at $\beta=t$ is obtained by Alfrey's rule[17] as the negative slope of relaxation modulus. In this paper, the relaxation spectra of solid polymeric materials were obtained by the following second approximation according to the method of Ferry and Williams[18].

$$H_2(\beta)=\frac{H_1(\beta)}{\Gamma(1+m)} \quad (25)$$

Where $-m$ is the slope of a double logarithmic plot of H against β; Γ is the well known gamma function. The procedure was to make a tentative calculation of H by setting $1/\Gamma(1+m)=1$ in Eq. (25). Form a tentative logarithmic plot of H against β, the slope $-m$ was measured at each point, and the corresponding values $1/\Gamma(1+m)$ was obtained and multiplied by the provisional value of H.

The relaxation spectra of solid polymers have been computed by making use of computer software programed by the authors. The relaxation spectra of nylon 6 monofilament fibers in air, water and electrolyte aquous solution at 10℃, 20℃, 30℃ and 40℃ were shown in Figure 6-8. As the temperature increases, the maximum of relaxation spectrum decreases greatly and the flow segments distribute in wider relaxation times scale. Their maxima represent concentrations of relaxation processes in certain regions of the logarithmic time scale.

Figures 9-12 show the lnβ versus $H(\beta)$ curves, at different temperatures, for the Nylon 6 monofilament fiber in air, H_2O and various electrolyte solutions. The relaxation spectra on Nylon 6 in various solvents shift to lower relaxation times in the order of air, H_2O, 0.5 M KCl, 0.5 M $BaCl_2$, and 0.5 M

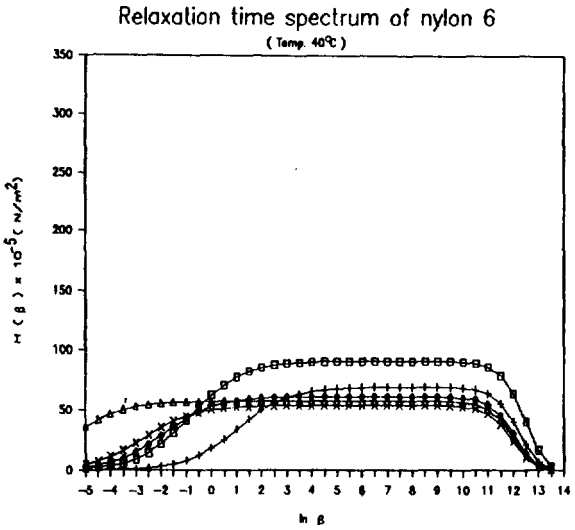

Figure 12. Relaxation time spectra of nylon 6 monofilament fibers in Air (□), H_2O (+), 0.5 M KCl (◇), 0.5 $BaCl_2$ (△) and 0.5 M $AlCl_3$ (x) at 40℃.

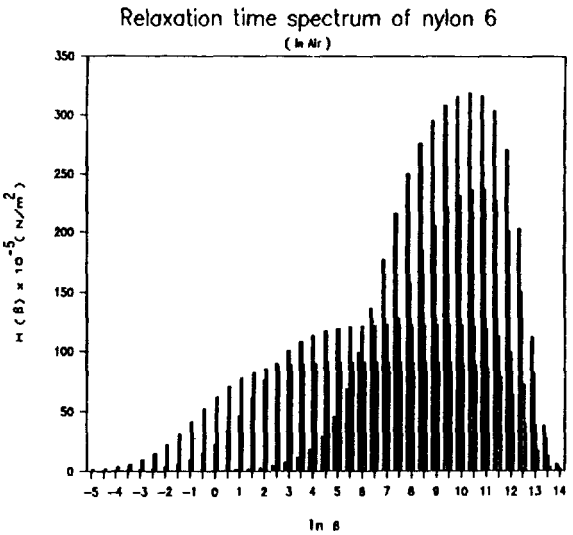

Figure 13. Relaxation time spectrum for a stress relaxation master curve of nylon 6 monofilament fibers in air.

$AlCl_3$ electrolyte aquous solution. As the swelling effect of the electrolyte aquous solution increases, the maximum of relaxation spectrum shifts to shorter relaxation times and decreases to lower intensity slightly. This notation means that the hydrogen bonding between adjacent molecules of nylon 6 is weakened by the swelling of electrolyte solutions. At the results, it may be assumed that the addition of electrolyte to the water, in which the nylon 6 fibers were stretched, accelerates the disintanglement of entangled flow segments and promotes the breaking of hydrogen bonds between the flow segments.

Figures 13, 14 show the relaxation spectra for the master relaxation curves of Nylon 6 filament fibers. Distributions of relaxation times for real polymer systems are complex as shown in the relaxation spectra for the master relaxation curves.

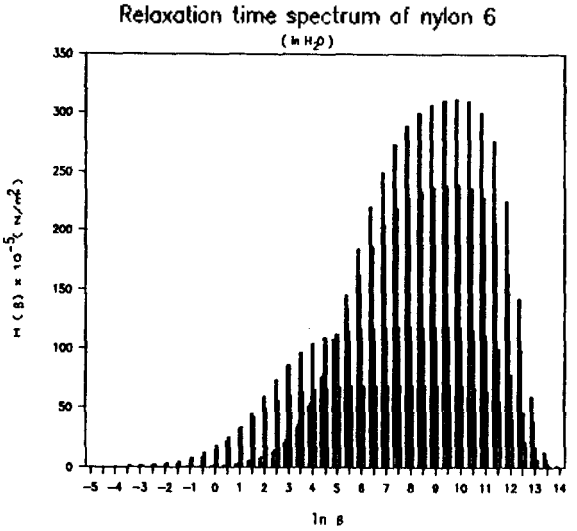

Figure 14. Relaxation time spectrum for a stress relaxation master curve of nylon 6 monofilament fibers in H_2O.

Table 1. The Values of Relaxation Spectra $H(\beta)$ Calculated from Stress Relaxation Curves for Nylon 6 in Air, H_2O, 0.5 M KCl, 0.5 M $BaCl_2$ and 0.5 M $AlCl_3$ Aqueous Solution at 20℃

	$H(\beta)\times10^{-5}$ (N/m²)				
β(sec)	Air	H_2O	0.5 M KCl	0.5 M $BaCl_2$	0.5 M $AlCl_3$
0.14	0.020	0.173	0.101	0.295	0.292
0.37	0.055	0.471	0.275	0.799	0.793
1.00	0.150	1.275	0.746	2.157	2.140
2.72	0.407	3.433	2.016	5.765	5.714
7.39	1.105	9.096	5.395	14.983	14.822
20.09	2.980	23.132	14.075	36.420	35.875
54.59	7.925	53.613	34.519	77.196	75.448
148.41	20.259	104.659	74.395	132.325	128.022
403.43	48.217	162.490	130.387	180.856	173.448
1096.63	97.578	205.154	181.749	209.772	200.130
2980.96	157.864	227.514	213.322	223.034	212.269
8103.08	205.561	236.893	227.858	228.107	216.874
12026.47	231.016	238.894	213.893	228.038	216.649
59874.14	236.121	228.019	210.479	214.241	203.007
162754.79	201.141	163.811	152.086	143.053	133.773
442413.39	81.433	38.461	31.383	26.909	24.204
1202604.28	4.052	0.508	0.302	0.206	0.168

Tables 1, 2 show the values of relaxation spectra $H(\beta)$ calculated from stress relaxation curves for nylon 6 filament fiber in various solutions at various temperatures. The general molecular concept has been applied qualitatively in various cases, and has been extended to explain the properties of materials which exhibit a distribution of relaxation times. If the sample is held in a deformed shape at constant tensile strain, the bond breaking and reforming will result in stress relaxation. The presence of bonds of different strengths and hence different rate constants for breaking and reforming result in the distribution of relaxation times, rather than a single relaxation time.

Table 2. The Values of Relaxation Spectra $H(\beta)$ Calculated from Stress Relaxation Curves for Nylon 6 in Air at 10℃, 20℃, 30℃ and 40℃

		$H(\beta)\times10^{-5}$ (N/m²)			
ln β	β (sec)	10℃	20℃	30℃	40℃
−2	0.14	0.049	0.020	3.756	21.601
−1	0.37	0.132	0.055	9.663	41.231
0	1.00	0.359	0.150	22.971	62.492
1	2.72	0.973	0.407	46.772	77.536
2	7.39	2.631	1.105	76.241	85.220
3	20.09	7.048	2.980	99.923	88.476
4	54.59	18.435	7.925	113.113	89.743
5	148.41	45.482	20.259	118.957	90.218
6	403.43	99.144	48.217	121.275	90.359
7	1096.63	176.509	97.578	122.151	90.458
8	2980.96	249.591	157.864	122.469	90.472
9	8103.08	295.495	205.561	122.528	90.402
10	22026.47	316.217	231.016	122.117	89.833
11	59874.14	316.939	236.121	118.867	85.805
12	162754.79	269.696	201.141	98.893	63.782
13	442413.39	111.932	81.433	38.555	16.802
14	1202604.28	5.937	4.052	1.808	0.917

References

1. R. H. Blanc, *Rheol. Acta.*, **27**, 482 (1988).
2. J. D. Ferry, *Viscoelastic Properties of Polymers*, Wiley, New York (1980).
3. B. H. Bersted, *J. Appl. Polym. Sci.*, **19**, 2167 (1975).
4. M. Shida and R. N. Shroff, *Trans. Soc., Rheology*, **14**, 605 (1970).
5. R. S. Lakes and S. Saha, *Science*, **104**, 501 (1979).
6. R. S. Lakes and J. L. Katz, *J. Biomech.*, **104**, 501 (1979).
7. N. W. Tschoegl, *Rheol. Acta*, **10**, 595 (1971).
8. J. Stanislav and B. Hlavacek, *Trans. Soc. Rheol.*, **17**, 331 (1973).
9. T. L. Smith, *J. Polym. Sci.*, **C35**, 39 (1971).
10. T. Ree and H. Eyring, *J. Appl. Phys.*, **26**(7), 793 (1955).
11. N. J. Kim, E. R. Kim, and S. J. Hahn, *Bull. Korean Chem. Soc.*, **12**, 468 (1991).
12. T. Kunugi, I. Isobe, and K. Kimura, *J. Appl. Polym. Sci.*, **24**, 923 (1979).
13. V. B. Gupta, C. Ramesh, and A. K. Gupta, *J. Appl. Sci.*, **29**, 4203 (1984).
14. N. W. Tschoegl, *The Theory of linear Viscoelatic Behavior*, Academic Press. New York (1981).
15. F. R. Schwarzl, *Pure Appl. Chem.*, **23**, 219 (1970).
16. F. R. Schwarzl, *Rheol. Acta*, **9**, 382 (1970).
17. T. Alfrey and P. Doty, *J. Appl. Phys.*, **16**, 700 (1945).
18. J. D. Ferry and M. L. Williams *J. Colloid Sci.*, **7**, 347 (1952).

Conducting Polypyrrole Doped with Hexacyanoferrate Anions: an Electrochemical and Spectroscopic Study

Junghee Han†, Seungjun Lee‡, and Woon-kie Paik*

Department of Chemistry, Sogang University, Seoul 121-742. *Received March 20, 1992*

Conducting polypyrrole doped with iron (II, III) hexacyanate $Fe(CN)_6^{4-}$ ions was studied for its physical and electrochemical properties. The polymer exhibited two pairs of waves in the cyclic voltammogram, one for the reversible oxidation/reduction of the incorporated iron hexacyanate ions and the other for the near-reversible oxidation/reduction of the polypyrrole moiety. The exchange of ions incorporated in the polymer and other ions present in solutions were examined by following the decrease of the reversible redox peaks of $Fe(CN)_6^{4-}$, and by EDX analysis. The spin density of this highly conducting polymer as probed by ESR spectroscopy was extremely low compared to polypyrrole doped with common anions.

Introduction

Conducting Polymers "doped" with various anions have attracted much interest in recent years. Although the main characteristics of a conducting polymer is determined by the kinds of monomers and the linkage between the monomers in the polymer backbone, the doped anions sometimes impart significant influence on the physical and electrochemical properties of the conducting polymers.[1] While most of the anions are chemically inert charge compensators in the polymer structure with the polymer itself in the cationic from, anions with multiple oxidation states may actively participate in the oxidation/reduction reaction. Polymers with such anions,

† Present address: Central Research Laboratory, Korea Explosives Group, Taejon 302-345, Korea
‡ Present address: R&D Department, Isu Chemical Company, Ltd., Onsan, Kyungnam 689-890, Korea